LWT - Food Science and Technology 244 (2026) 119206

Contents lists available at ScienceDirect

LWT

journal homepage: www.elsevier.com/locate/lwt

Dark chocolates: Effects of emulsifier types and concentrations on physico-mechanical properties

Barbora Lapčíková [a,b], Lubomír Lapčík [a,b,*], Vojtěch Neuwirth [b], Erick Omodho Okelo [b], Tomáš Valenta [b], Martin Vašina [c,d], David Řepka [a], Aneta Machalová [b]

[a] Department of Physical Chemistry, Faculty of Science, Palacky University, 17. Listopadu 12, Olomouc, 771 46, Czechia
[b] Tomas Bata University in Zlin, Department of Food Technology, Faculty of Technology, Nam. T. G. Masaryka 275, Zlin, 762 72, Czechia
[c] Tomas Bata University in Zlin, Department of Physics and Materials Engineering, Faculty of Technology, Nam. T. G. Masaryka 275, Zlin, 762 72, Czechia
[d] VSB-Technical University of Ostrava, Department of Hydromechanics and Hydraulic Equipment, Faculty of Mechanical Engineering, 17. Listopadu 2172/15, Ostrava-Poruba, 708 00, Czechia

ARTICLE INFO

Keywords:
Dark chocolate
emulsifier
Casson plastic viscosity
PSD
Bending properties
Acoustic emissions

ABSTRACT

This study investigated the effects of post-conching blending with various emulsifiers on the physico-mechanical and sensory properties of dark chocolate. Polyglycerol polyricinoleate (PGPR), mono- and diglycerides (MD), soya lecithin (LSO) and sunflower lecithin (LSL) in three different concentrations were used. After conching, the emulsifier was mixed with 500 g of chocolate at a temperature of 50 °C and 500 rpm for 30 min using the Thermomix TM 6 mixer. The chocolates were evaluated in terms of particle size distribution, bending, acoustic, rheological, melting, colour and sensory properties. All emulsified chocolates exhibited reduced Casson plastic viscosity (η_c) compared to the conched (STAN) and blended (MIX) samples, with the exception of PGPR_0.50. PGPR and MD showed higher viscosity values compared to lecithin samples. With increasing emulsifier concentration, a decrease in yield stress and thixotropy was observed for PGPR samples, while MD samples exhibited an increase in these parameters. In lecithin samples, a decrease in rheological parameters was observed up to the concentration of 0.50 w.%, while an increase in η_c at 1.00 w.% was found. Particle size analysis revealed higher volume diameters *Dv(90)* for MD and PGPR samples (ranging from 18.60 to 23.30 μm) compared to LSO and LSL samples (from 18.30 to 19.00 μm). The melting temperature of the studied chocolates was determined using differential scanning calorimetry (DSC). In addition, cocoa butter polymorphs were observed using modulated DSC (MDSC).

1. Introduction

Dark chocolate belongs to the most popular snacks due to its pleasant taste, aroma and texture (Gómez-Fernández et al., 2021). European Union legislation defines dark chocolate as a confectionary product composed of at least 35% of cocoa mass, 18% of cocoa butter and 14% of dry non-fat cocoa solids with addition of any sugar (Saputro, Van de Walle, Kadivar, et al., 2017). Over the years, scientists have focused on formulation and processing aspects to produce nutritional and sensory attributes (Muhammad et al., 2018). In chocolates processing, there are four fundamental processing steps: mixing, refining, conching and tempering (Pombal et al., 2024). Conching presents a significant step determining the flavour and texture of chocolates. It refers to the process, in which the chocolate ingredients undergo gradual heating ($T >$ 40 °C), mixing, shearing and aeration to obtain homogenous viscous suspension (Beckett et al., 2017). Conching process transforms the dry ingredients into plastic-like suspension and finally to a liquid upon the addition of cocoa butter and/or emulsifier (Guckenbiehl et al., 2024). Plastic conching facilitates taste and flavour development (Albak & Tekin, 2016). It also enhances the dispersion of cocoa and sugar solids in a continuous fat phase resulting in decreased solid-solid interaction and viscosity. Conching temperature, equipment and the moisture content of the dry ingredients influence the resulting product texture and sensory characteristics (Guckenbiehl et al., 2024; Toker et al., 2019). Although blending process has been used in food industry for decades, its application in chocolate processing is still low and not very well understood. Blending is a gentle mixing process aimed at creating an intact soli-solid particle interaction with or without the involvement of the liquid phase

* Corresponding author. Department of Physical Chemistry, Faculty of Science, Palacky University, 17. Listopadu 12, Olomouc, 771 46, Czechia.
E-mail address: lubomir.lapcik@upol.cz (L. Lapčík).

https://doi.org/10.1016/j.lwt.2026.119206
Received 2 September 2025; Received in revised form 23 January 2026; Accepted 27 February 2026
Available online 28 February 2026

(Bhandari et al., 2025). Blending results in the breakdown and redistribution of particles and an increase in packing density with consequent decrease in Casson plastic viscosity of the chocolate melt (Rohm et al., 2018).

In addition to the unit operations, emulsifiers play a critical role in determining the stability, aroma, flow behaviour, appearance and texture of dark chocolates (Toker et al., 2019). Emulsifiers adsorb on the surfaces of cocoa and sugar particles, which are suspended in a fat phase. Thereby, emulsifiers reduce agglomeration of these particles and increase flowability of the molten chocolate (Pombal et al., 2024; Sözeri Atik et al., 2020; Toker et al., 2024). Polyglycerol polyricinoleate (PGPR) and lecithins belong to commonly used emulsifiers. On the other hand, lecithin is associated with changes in yield stress, plastic viscosity and crystallization behaviour of fats in chocolate, which mainly depends on its concentration (Pombal et al., 2024; Sözeri Atik et al., 2020). Lecithin facilitates the dispersion of solid particles, such as sugar and cocoa components, into the fat phase. Owing to their amphiphilic character and medium hydrophilic-lipophilic balance (HLB) (7–9), lecithins can behave as both O/W (oil/water) and W/O emulsifiers depending on the colloidal system type. However, in fat-based systems such as chocolate, they act predominantly at the particle-fat interface. PGPR is strongly lipophilic (HLB 1–3), which accounts for its pronounced ability to reduce interfacial tension in chocolate. Although it serves as a W/O emulsifier, it primarily acts in chocolate as a structural modifier of the fat phase. Mono- and diglycerides of fatty acids (MD and non-ionic emulsifier, E471) have lower HLB value (3−5) and allow the stabilization of the fat phase by controlling the fat crystallization in the chocolate.

Despite the widespread use of PGPR, lecithins, and MD, previous studies have widely focused on traditionally conched systems. The combined effects of a post-conching blending step and varying emulsifier types and concentrations have not been systematically evaluated. This is one of the first studies that systematically evaluates the effect of selected emulsifiers (PGPR, lecithins, and MD) on physico-mechanical properties of a blended dark chocolate system. The aim of this study was to: (1) investigate the effects of incorporating a blending step after conching on the physico-mechanical properties of dark chocolates; (2) examine how the type and concentration of selected emulsifiers (PGPR, mono- and diglycerides, soya lecithin, and sunflower lecithin) modify these functional properties; and (3) assess the sensory implications of these changes to identify experimentally supported concentration ranges providing advantageous technological and organoleptic performances.

The novelty of this study lies in: (1) introducing a blending operation after conching and quantifying its impact on flow behaviour, particle size distribution, mechanical-acoustic and melting properties, colour and sensory analyses; (2) evaluating how emulsifiers act under these modified processing conditions; and (3) providing a direct comparison between standard conched (STAN) and blended (MIX) chocolates. This integrated approach enables the identification of emulsifiers' concentration ranges in blended dark chocolate, a perspective that has not yet been reported in the literature. Another aspect represents the systematic assessment of four different emulsifier types across multiple concentrations, using multi-modal assessment including principal component analysis (PCA).

2. Materials and methods

2.1. Chocolate recipe ingredients

Commercially available food-grade ingredients were used for chocolate preparation. The cocoa mass was sourced from Trinitario cocoa beans, Costa Rica. A cold-pressed and deodorized cocoa butter was sourced from Peru. Both ingredients were delivered by Vital Country LTD. (Pilsen, Czechia). Extra fine powdered sugar was purchased from Agrana Sales & Marketing GmbH. (Tulln an der Donau, Austria). Sunflower lecithin (LSL) and soya lecithin (LSO) in powder forms were delivered by Green Medical, LTD. (Prague, Czechia). Polyglyceryl-3 Polyricinoleate and Polyglyceryl-3 Ricinoleate (PGPR) (brand named "Neocare P3R″, batch No. 7398) was obtained from Nature-Store (Ústí nad Labem, Czechia), and mono- and diglycerides of fatty acids (MD) as a glyceryl monostearate and glyceryl distearate mixture from J. K. Food LTD. (Větřkovice, Czechia).

2.2. Preparation of dark chocolate samples

55 g of cocoa mass, 10 g of cocoa butter and 45 g of sugar were grounded followed by conching at the temperature range from 60 to 70 °C (Spectra 11 melanger, New York, NY, USA) for 7 h to obtain chocolate liquor with a particle size < 30 μm, determined using a digital micrometre (Mitutoyo No. 293-821-30, Mitutoyo Corporation, Kawasaki, Japan). The resulting chocolate liquor was tempered by cooling to 28 °C, followed by heating to 32 °C and finally moulded to obtain the STAN sample (Table 1).

A blending step was incorporated into the above procedure after conching to obtain the MIX sample, and was conducted at 50 °C for 30 min at a rotational speed of 500 rpm using Thermomix TM 6 mixer (Vorwerk SE KG, Wuppertal, Germany). The blending was defined as a short, post-conching, high-shear mixing stage applied under fixed time, temperature, and rotor-speed conditions, distinct from prolonged wet conching.

To obtain the emulsified chocolate samples, the above procedure used for the MIX sample was adopted with the addition of different emulsifiers (PGPR, MD, LSO and LSL) of prescribed doses (Table 2) for each chocolate preparation during blending. The samples were then stored at 20 °C until analysis. The flow diagram illustrating the sample preparation design and analyses is shown in Fig. 1.

2.3. Sample analysis

2.3.1. Moisture content

The moisture content was determined (in triplicate) following the procedure of Neuwirth et al. (Neuwirth et al., 2024) with minimal modifications. Briefly, 5 g of the chocolate sample was added to a metallic container filled with pre-dried sand and their total weight taken (m_i). The sample mix was subsequently dried at 98 °C in hot air oven (Stericell 55 Standard, BMT Medical Technology, Czechia) for 12 h followed by weighing of the dry mass (m_f). The percentage moisture content (m_c) was determined as the loss in weight at the end of drying according to Eq. (1):

$$m_c = \left(1 - \frac{m_f}{m_i}\right) * 100 \quad (1)$$

2.3.2. Particle size distribution (PSD) analysis

PSD and specific surface area were determined using Malvern Mastersizer 3000 laser diffraction particle size analyser (Malvern Instruments Ltd, Worcestershire, UK) following the procedure (Saputro, Van de Walle, Aidoo et al., 2017) with a few modifications. Briefly, chocolate samples were first grated, dispersed in isopropanol (50 mg/mL) and heated at 55 °C for 1 h. To standardize the sizes of particles

Table 1
Composition of the standard (STAN) chocolate mass.

Composition (w.%)	
Cocoa mass	53.4 ± 0.1
Sugar	43.6 ± 0.1
Cocoa butter	3.0 ± 0.1
Total fat	32.4 ± 0.5
Moisture	1.11 ± 0.03

Note: Values of total fat content and moisture content are presented as mean ± SD of three analyses.

Table 2
Studied chocolate samples labelling.

Sample labelling	Emulsifier type	Emulsifier content (w.%)	Moisture content (w. %)
PGPR_0.10	Polyglycerol polyricinoleate (PGPR)	0.10	1.38 ± 0.08^{abc}
PGPR_0.25		0.25	1.32 ± 0.03^{ace}
PGPR_0.50		0.50	1.48 ± 0.01^{b}
MD_0.50	Mono- and diacylglycerides of fatty acids (European designation for a food additive approved for use in the EU: E471)	0.50	1.41 ± 0.01^{ab}
MD _0.75		0.75	1.38 ± 0.07^{abc}
MD _1.00		1.00	1.37 ± 0.10^{abc}
LSO_0.20	Soya lecithin (LSO)	0.20	1.19 ± 0.02^{de}
LSO_0.50		0.50	1.14 ± 0.01^{df}
LSO_1.00		1.00	1.22 ± 0.01^{de}
LSL_0.20	Sunflower lecithin (LSL)	0.20	1.19 ± 0.01^{de}
LSL_0.50		0.50	1.26 ± 0.05^{cef}
LSL_1.00		1.00	1.25 ± 0.01^{cef}
STAN (standard)	_	0	1.11 ± 0.03^{d}
MIX (blended standard)	_	0	1.36 ± 0.02^{abc}

Note: The reference sample, labelled "MIX", was prepared through the blending process and used as the chocolate mass in the emulsified formulations. The analysed values are presented as mean ± SD of three measurements. Different superscript letters in the same column indicate statistically significant differences between the samples ($p \leq 0.05$, Tukey HSD test).

prior to measuring, the diluted samples were ultrasonicated at 80 Hz for 10 min prior to measurement. The samples were then loaded into the particle size analyser and measured at set parameters: particle refractive index (1.61), adsorption index (0.10), obscuration (9 − 10%) and suspension refractive index (1.38). The PSD was quantified as relative volume of particles in size bands: *Dv*(90, 50 and 10) representing 90, 50 and 10% percentiles. Sauter diameter *D[3,2]* was derived from the collected data. All the tests were performed in triplicates.

2.3.3. Rheological properties

The analysis of the flow behaviour was based on the procedure of (Saputro, Van de Walle, Aidoo et al., 2017) using concentric cylinder rheometer (Kinexus PRO, Malvern Pananalytical Ltd., Malvern, UK) with a gap of 9.15 mm. Briefly, the samples were heated in the oven at.

45 °C for 2 h. Samples were then pre-sheared at a shear rate ($\dot{\gamma}$) of 5 s^{-1} for 5 min. To measure the flow behaviour, a volume of 17.1 mL of the pre-sheared chocolate sample was loaded into the rheometer and sheared at an increasing $\dot{\gamma}$ from 2 to 50 s^{-1} (ramp-up), held at $\dot{\gamma}$ of 50 s^{-1} for 180 s and subsequently ramped down at a decreasing $\dot{\gamma}$ from 50 to 2 s^{-1}. The data from the ramp-up curve were subsequently fitted to the Casson model to derive Casson yield stress (τ_{0C}) and Casson viscosity (η_c) according to Eq. (2). Thixotropy was determined from the difference between the ramp-up and ramp-down shear stress curves. During the measurements, the temperature was kept at 40 °C to keep the sample in a molten state (Gallery et al., 2024).

$$\sqrt{\tau} = \sqrt{\tau_{0c}} + \sqrt{\eta_c \times \dot{\gamma}} \quad (2)$$

2.3.4. Uniaxial three-point bending test

The uniaxial three-point bending test was carried out on Universal Testing Machine (Autograph AGS-100 Shimadzu, Kyoto, Japan) according to the international standard (International Organization for Standardization, 1998). The distance between the supports was set to 64 mm. The loading velocity was 10 mm/min. Samples of chocolate bars with dimensions of (24.5 × 98.0 × 10.2) mm (width × length × thickness) were measured using a V-shaped R5 probe (5 mm radius), descending in a parallel manner on the centre of the bar (Severa, 2014; Zhao et al., 2018). The data were processed using the Trapezium X software (Shimadzu, Kyoto, Japan) to determine the mean maximum bending force (F_{max}) and the mean bending modulus of elasticity (E_B). All experiments were conducted at a temperature of 22 °C.

2.3.5. Acoustic measurement

Acoustic emissions generated during the manual fracture of studied chocolate bars were evaluated by measuring the sound pressure level L_p (dB), defined by Eq. (3):

$$L_p = 20 \cdot log_{10}\left(\frac{p}{p_0}\right) \quad (3)$$

Where p is the effective (root mean square) sound pressure (Pa), and p_0 is the reference sound pressure (Pa), i.e., 20 μPa in the air atmosphere (Anicic et al., 2016; Lapčíková et al., 2022).

The peak A-weighted sound pressure levels L_{pAmax} (dB), which accurately reflect the sensitivity of human ears (Staiano, 2007), were experimentally detected using a Voltcraft SL-400 sound level meter (Conrad Electronic SE, Hirschau, Germany) in an acoustic chamber. The chocolate samples were broken in close proximity to the microphone sensor of the sound level meter.

2.3.6. Thermal properties

The melting behaviour of studied chocolates was determined by Differential Scanning Calorimeter (DSC) (Discovery DSC 250, TA Instruments-Waters LLC, New Castle, DE, USA). Approximately 5 mg of a chocolate sample was loaded into aluminium pans, hermetically sealed and equilibrated overnight at 25 °C. An empty aluminium pan was used as a reference. The sample and reference pans were loaded into DSC equipment and heated from 5 to 50 °C (Indiarto et al., 2024) at the heating rate of 5 °C/min, while measuring the heat flux required to increase the temperature of the sample over time (Saputro, Van de Walle, Aidoo et al., 2017). The instrument was calibrated for indium standard (T_m = 156.6 °C; ΔH = 28.45 J/g). The obtained thermal data were processed using TA Universal Analysis 2000 Software (Version 4.5A, TA Instruments-Waters LLC, New Castle, DE, USA) to obtain the onset melting temperature (T_o), peak melting temperature (T_p) and the enthalpy change (ΔH) of the chocolates. The measurements were performed in triplicates.

Temperature modulated differential scanning calorimetry (MDSC) was also performed on DSC 250 Discovery instrument (TA Instruments, New Castle, DE, USA) (Lapčík et al., 2022). Chocolate samples of (5.0 ± 0.1) mg were weighed into non-hermetic aluminium pans and sealed with an aluminium lid. An empty aluminium pan was used as a reference. The measurement was realized in a nitrogen atmosphere at the flow rate of 50 ml/min. MDSC was conducted using modulated temperature 1 °C/120 s in the temperature range of 0 − 50 °C with the heating rate of 2 °C/min. The temperature peaks related to cocoa butter melting were expressed as onset melting temperature T_o and peak melting temperature T_p. Heat of fusion was calculated by integrating the area under the thermogram and expressed as melting enthalpy ΔH. Reversing and non-reversing heat flows were used to split the endothermic melting peaks, representing heat capacity component (reversing curve) and kinetic component (non-reversing curve) (Leyva-Porras et al., 2020; Tolstorebrov et al., 2014).

2.3.7. Colour analysis

Colour analysis of dark chocolates was performed by the Spectro-

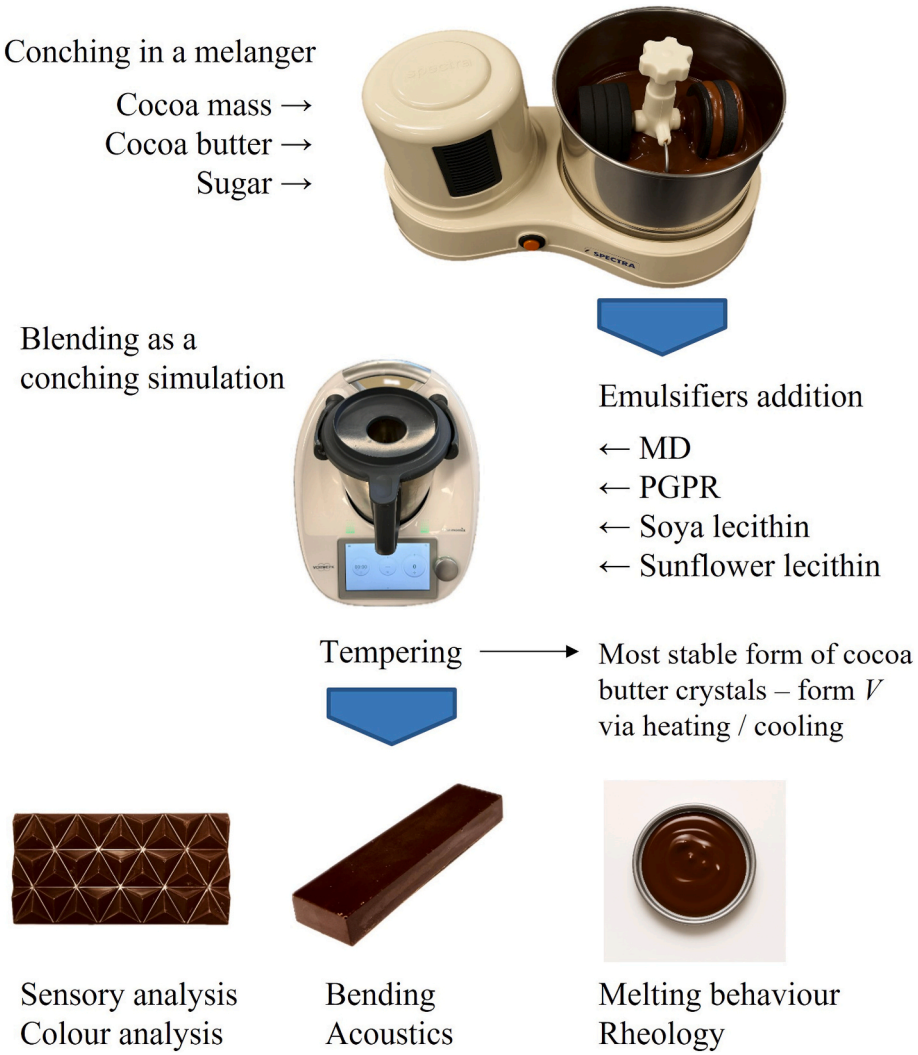

Fig. 1. Flow diagram illustrating the sample preparation design and analyses.

photometer UltraScan VIS (Hunter Associates Laboratory, Inc., Reston, VA, USA). Measurements were realized using an Illuminant D65/10 (standard daylight with 10° angle) operating in RSIN (reflectance specular-included) mode. Diffusive 8 Instrument Standard from titanium dioxide was used as a reference. Samples of cone-shaped chocolates were measured after removing from polypropylene cups, attached to the sensor from quartz glass. The CIE $L^*a^*b^*$ uniform colour space was applied to determine the chocolates' lightness L^* (0 = black; 100 = white), chromaticity coordinates a^* (from the greenness (−) to redness (+)), and b^* (from the blueness (−) to yellowness (+)). Three experiments were performed for each sample analysed in three replicates. To assess the colour profile of the samples, hue angle h^* ($h^* = tan^{-1}$ (b^*/a^*)), and colour saturation, i.e., chroma C^* ($C^* = (a^{*2} + b^{*2})^{1/2}$) were determined (Lapčíková et al., 2024). Differences between the samples and the STAN as the relevant reference were evaluated by the total colour difference ΔE^*. This parameter was applied to identify the inconsistencies in samples' colour profile, i.e., the levels of colour perceptibility by human eyes. The total colour difference was calculated as follows (Brainard, 2003):

$$\Delta E^* = \sqrt{\left(L_2^* - L_1^*\right)^2 + \left(a_2^* - a_1^*\right)^2 + \left(b_2^* - b_1^*\right)^2} \quad (4)$$

2.3.8. Sensory analysis

To determine the sensory attributes of the dark chocolate preparations, a sensory test panel consisting of 11 adults aged (20 − 60) years old were selected and trained according to EN ISO 8586:2023 guidelines (International Organization for Standardization, 2023). The panellists were provided with 5 g of each selected sample, a glass of clear water, an informed consent form, and a sample evaluation protocol. Each panellist was asked to rank the chocolate samples based on colour, hardness, melting in the mouth, flavour, aroma and overall acceptability. From assessing one sample to the next, the panellists rinsed their mouths three times with clear water and waited for 1 min. The sensory attributes were ranked on a 5-point hedonic scale where 1 – Dislike extremely, 2 – Dislike slightly, 3 – Neither like nor dislike, 4 – Like slightly, and 5 – Like extremely.

2.4. Statistical analysis

The data are presented as mean ± standard deviation (SD) of three measurements in both tables and figures. Significant differences among sample means were assessed at 5% significance level using a one-way ANOVA and Turkey's HSD test for post-hoc analysis. Sensory data were statistically evaluated using the Friedman test and Nemenyi test to verify the compliance of a sensory preference level. Principal component analysis (PCA) was performed using R software (version 4.5.1; R Foundation for Statistical Computing, Vienna, Austria) to explore multivariate relationships among the functional parameters (F_{max}, E_B, η_c, τ_{0C}, and L_{pAmax}) of chocolate samples.

3. Results and discussion

3.1. Particle size distribution (PSD)

The particle size of dispersed cocoa components and sugar in the studied chocolate samples was determined as a volume particle size distribution (PSD). The observed particle size distribution functions of the studied chocolate dispersions are shown in Fig. S1 (Appendix A1, Supplementary Material). The resulting PSD parameters, including $D_V(90)$, $Dv(50)$, $Dv(10)$, the Sauter mean diameter $D[3,2]$, and the specific surface area of the chocolate samples, are summarised in Table 3 and revealed the effects of individual emulsifiers in the chocolate formulations. Owing to the predominant dissolution of the fat phase in isopropanol, the obtained results reflect the particle sizes of the dispersed cocoa components and sugar.

The $Dv(90)$ value of the STAN sample was 17.10 ± 0.28 μm, while that of the MIX sample reached 20.10 ± 0.41 μm. The higher $D_V(90)$ observed for MIX is related to increased migration of water to the surface of dispersed sugar particles, leading to their aggregation and to a higher moisture content of 1.36 ± 0.02% (Table 1) (Suri & Basu, 2022). Lower $D_V(90)$ values were observed for lecithin-containing samples compared to samples containing PGPR and MD. Lecithin-modified samples exhibited particle sizes ranging from 18.30 ± 0.30 μm (LSL_0.20) to 19.0 ± 0.25 μm (LSO_0.50). The blending process confirmed that lecithins primarily adsorb on the surface of sugar particles and contribute to refinement of the chocolate structure (Ziegler et al., 2003)

MD and PGPR showed relatively higher $D_V(90)$ values as a result of interactions between the emulsifier and the fat crystalline structure, which likely promoted increased sugar aggregation during blending, as also evidenced by the comparison between the STAN and MIX samples. With respect to concentration dependence, a decreasing trend in $D_V(90)$ with increasing emulsifier concentration was observed for both PGPR and MD, except for the PGPR_0.50 sample, where a reduction in $Dv(90)$ to 18.60 ± 0.26 μm was recorded. The PSD values were directly proportional to the Sauter mean diameter and inversely proportional to the specific surface area. The Sauter mean diameter $D[3,2]$ ranged from 3.75 ± 0.07 μm (LSO_0.20) to 4.68 ± 0.06 μm (MIX), while the specific surface area increased from 0.97 ± 0.02 m^2/g (MIX) to 1.21 ± 0.02 m^2/g (LSO_0.20).

3.2. Rheological behaviour

Dark chocolate as a solid suspension of sugar and cocoa particles in cocoa butter showed non-Newtonian flow behaviour, as shown in Fig. 2 (Kadivar et al., 2016). The Casson model was fitted to the flow curves to study the Casson yield stress and Casson plastic viscosity. Yield stress was evaluated in regard to the energy amount required to initiate chocolate flow, and plastic viscosity to the energy needed to maintain the flow. Both STAN (conched only) and MIX (blended) samples were included as reference formulations to quantify the extent, to which the blending step modifies the response of chocolate to different emulsifier types and concentrations. As reported by Biswas et al. (Biswas et al., 2017), high-viscous chocolates are not desirable due to a sticky mouth-feel. In the present study, a decreasing trend in Casson plastic viscosities compared to STAN and MIX (with Pearson correlation coefficient of Casson model fit about ≈1.0) was observed for all emulsifiers applied, as shown in Fig. 3A.

Lecithin samples exhibited a significant decrease in η_c compared to MIX and STAN across all studied concentrations (Table 4). However, at the concentrations of 0.20 and 0.50 w.%, a further decline in η_c was observed. A similar rheological behaviour was reported by Pombal et al. (Pombal et al., 2024), who observed a decrease in chocolate plastic viscosity with increasing lecithin concentrations up to 0.60 w.%. According to Caparosa and Hartel, the incorporation of 0.50 w.% lecithin led to a viscosity reduction comparable to that achieved by adding approximately 5 w.% of cocoa butter (Caparosa & Hartel, 2020). For 1.00 w.% lecithin concentration (LSO_1.00 and LSL_1.00), the increase in plastic viscosity was found. It can be attributed to the formation of reverse micelles within the continuous fat phase (Garti & Aserin, 2012). Beckett and Afoakwa predicted the formation of multilayer structures surrounding dispersed sugar particles (Afoakwa, 2016; Beckett, 2008, p. 240).

The addition of lecithin (LSO_0.20 and LSL_0.20 samples) significantly reduced the yield stress. However, as shown in Fig. 3B, yield stress increased with lecithin concentrations from 0.20 to 1.00 w.%. This observation aligns with previous reports indicating an increase in chocolate yield stress, particularly at lecithin concentrations of approximately from 0.30 to 0.50 w.% (Glicerina et al., 2016; Vavreck, 2004).

For PGPR and MD samples, there was found an increase in Casson plastic viscosity with the elevated emulsifier concentration. Compared to STAN, a reduction in η_c was observed at PGPR concentrations ranging from 0.10 to 0.25 w.%. This indicates that PGPR improved chocolate flowability by reducing the initial resistance to flow. This behaviour reflects the ability of PGPR to disrupt particle-particle interactions and promote a more lubricated, weakly structured suspension (Afoakwa

Table 3
Particle size distribution (PSD) of chocolate samples (average data from volume-size distribution curves).

Samples	Specific surface area (m^2/g)	Particle diameters by volume			
		$D_V(10)$ (μm)	$D_V(50)$ (μm)	$D_V(90)$ (μm)	$D[3,2]$ (μm)
STAN	1.056 ± 0.018^{a}	1.90 ± 0.03^{ad}	7.04 ± 0.12^{a}	17.10 ± 0.28^{a}	4.29 ± 0.07^{ae}
MIX	0.968 ± 0.019^{a}	2.10 ± 0.06^{b}	7.83 ± 0.16^{b}	20.10 ± 0.41^{b}	4.68 ± 0.06^{b}
PGPR_0.10	1.038 ± 0.013^{a}	1.84 ± 0.05^{af}	7.43 ± 0.13^{c}	22.10 ± 0.29^{c}	4.38 ± 0.05^{a}
PGPR_0.25	1.036 ± 0.016^{a}	1.80 ± 0.04^{af}	7.50 ± 0.11^{c}	21.90 ± 0.27^{c}	4.43 ± 0.05^{ac}
PGPR_0.50	1.049 ± 0.017^{a}	2.01 ± 0.05^{bd}	7.51 ± 0.10^{c}	18.60 ± 0.26^{ef}	4.23 ± 0.09^{ae}
MD_0.50	1.004 ± 0.015^{a}	1.90 ± 0.02^{ad}	7.70 ± 0.14^{c}	23.30 ± 0.38^{d}	4.51 ± 0.05^{bc}
MD _0.75	1.015 ± 0.021^{a}	1.86 ± 0.04^{a}	7.63 ± 0.12^{c}	22.50 ± 0.23^{c}	4.50 ± 0.08^{bc}
MD _1.00	1.014 ± 0.018^{a}	1.89 ± 0.03^{a}	7.67 ± 0.14^{c}	20.40 ± 0.33^{c}	4.48 ± 0.09^{bc}
LSO_0.20	1.207 ± 0.022^{a}	1.53 ± 0.02^{c}	6.35 ± 0.14^{f}	18.40 ± 0.19^{eg}	3.75 ± 0.07^{d}
LSO_0.50	1.106 ± 0.016^{a}	1.66 ± 0.03^{e}	6.61 ± 0.11^{gf}	19.00 ± 0.25^{f}	4.10 ± 0.07^{ef}
LSO_1.00	1.204 ± 0.021^{a}	1.73 ± 0.04^{ef}	6.86 ± 0.10^{ag}	18.40 ± 0.21^{eg}	3.89 ± 0.06^{df}
LSL_0.20	1.117 ± 0.017^{a}	1.72 ± 0.03^{ef}	6.84 ± 0.13^{ag}	18.30 ± 0.30^{e}	4.07 ± 0.08^{e}
LSL_0.50	1.073 ± 0.014^{a}	1.82 ± 0.05^{af}	6.99 ± 0.11^{a}	18.80 ± 0.27^{fg}	4.22 ± 0.06^{ae}
LSL_1.00	1.095 ± 0.015^{a}	1.79 ± 0.03^{af}	6.91 ± 0.13^{a}	18.60 ± 0.22^{ef}	4.18 ± 0.05^{ae}

Note: $D_V(10)$ – effective volume diameter corresponding to 10% of cumulative distribution percentage (μm); $D_V(50)$ – mean volume diameter corresponding to 50% of cumulative distribution percentage (μm); $D_V(90)$ – volume diameter corresponding to 90% of cumulative distribution percentage (μm); $D[3,2]$ – Sauter mean diameter. The values are presented as mean ± SD of three measurements. Different superscript letters in the same column indicate statistically significant differences between the samples ($p \leq 0.05$, Tukey HSD test).

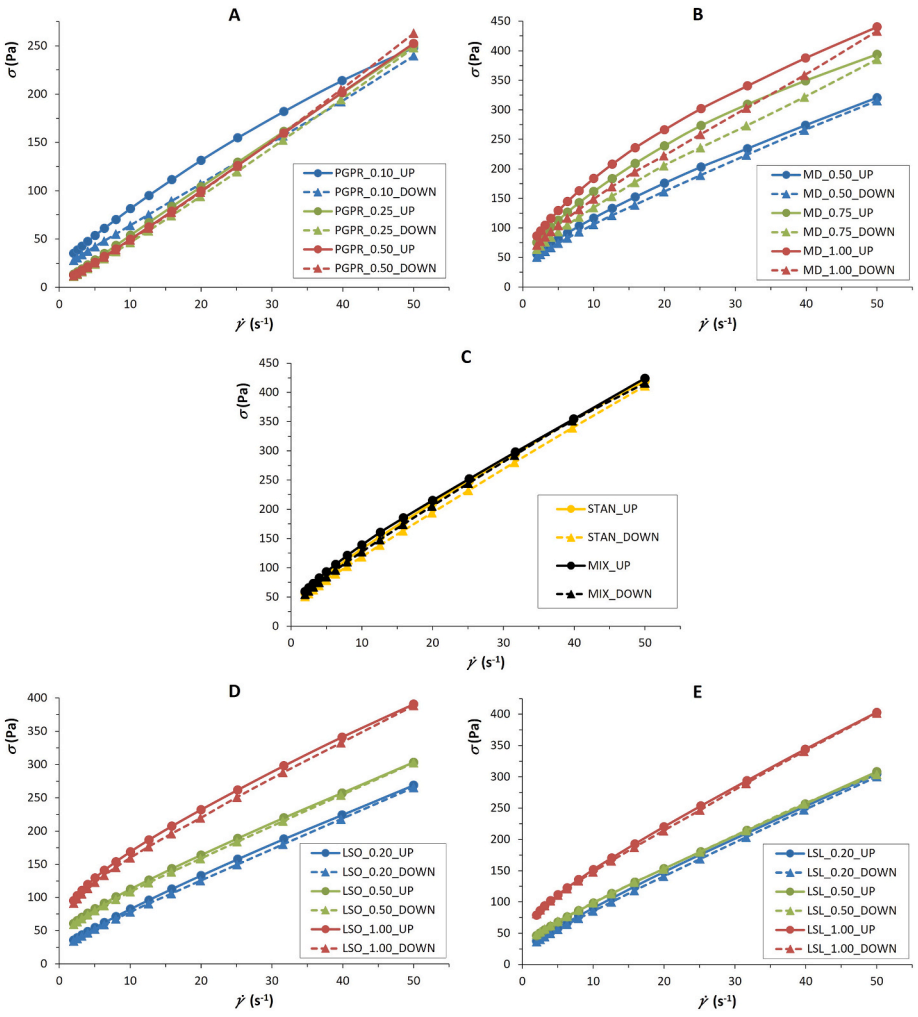

Fig. 2. Experimental flow curves of studied chocolate samples.

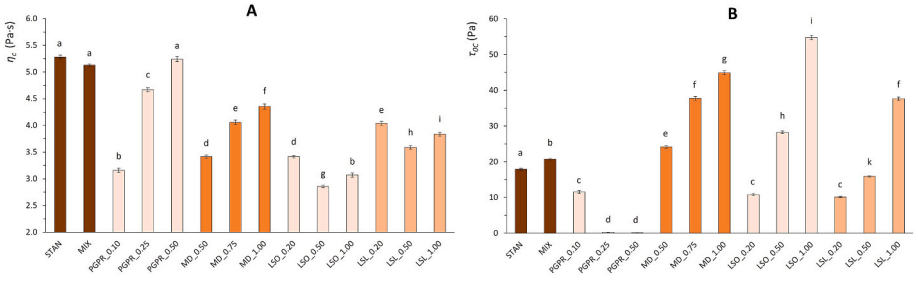

Fig. 3. Casson plastic viscosity η_c (part A) and yield stress τ_{0C} (part B) of molten chocolate. Different superscript letters above the error bars (standard deviations) indicate statistically significant differences between the samples ($p \leq 0.05$, Tukey HSD test).

et al., 2007; Garti & Aserin, 2012; Schantz & Rohm, 2005). For the PGPR_0.50 sample, the viscosity was comparable to that of STAN sample. A pronounced decrease in yield stress (τ_{0C}) was observed with increasing PGPR concentration (Fig. 3B). The highest τ_{0C} was found for the PGPR_0.10 sample, whereas at higher concentrations (PGPR_0.25 and PGPR_0.50), the yield stress was reduced to nearly zero. It is caused by adsorbing at solid-fat interfaces, lowering interparticle friction and facilitating flow, demonstrating the applicability of PGPR in achieving smoother and more efficient chocolate moulding and depositing (Afoakwa, 2016; Bastida-Rodríguez, 2013). MD chocolate samples exhibited an increase in yield stress with increasing emulsifier concentration compared to STAN and MIX. MD appears to promote fat crystal networking, contributing to a more structured fat phase. Therefore, the synergistic combination of the elevated τ_0 and the decreased η_c offers technological advantages for chocolate manufacturing.

The results of the thixotropy analysis are shown in Fig. 4. MIX sample exhibited significantly lower thixotropy ($p \leq 0.05$) compared to STAN, indicating that the blending enhanced internal cohesion and development of a more structurally stable and time-independent flow properties (Ziegler & Hogg, 2009). A significant reduction in thixotropy was observed for both lecithins at 0.50 w.% concentration. It can be concluded that the addition of lecithin contributes to chocolate's flow behaviour approaching time-independent characteristics (Servais et al., 2003). A reduction in thixotropy to negative values was observed for the

Table 4
Results of the Casson plastic viscosity flow curves fitting.

Samples	η_c (Pa·s)	τ_{OC} (Pa)	PCC (−)
STAN	5.283 ± 0.035^{a}	17.92 ± 0.31^{a}	1.0000
MIX	5.131 ± 0.021^{b}	20.74 ± 0.26^{b}	0.9999
PGPR_0.10	3.159 ± 0.044^{c}	11.56 ± 0.38^{c}	0.9997
PGPR_0.25	4.670 ± 0.038^{d}	0.27 ± 0.04^{d}	0.9999
PGPR_0.50	5.242 ± 0.050^{ab}	0.15 ± 0.03^{d}	0.9997
MD_0.50	3.416 ± 0.031^{e}	24.16 ± 0.40^{e}	0.9999
MD _0.75	4.060 ± 0.041^{f}	37.73 ± 0.59^{f}	0.9976
MD _1.00	4.357 ± 0.049^{g}	44.89 ± 0.55^{g}	0.9976
LSO_0.20	3.415 ± 0.027^{e}	10.80 ± 0.29^{cj}	0.9999
LSO_0.50	2.858 ± 0.024^{h}	28.27 ± 0.37^{h}	0.9997
LSO_1.00	3.072 ± 0.038^{c}	54.84 ± 0.60^{i}	0.9999
LSL_0.20	4.040 ± 0.041^{f}	10.14 ± 0.22^{j}	0.9999
LSL_0.50	3.588 ± 0.033^{i}	15.97 ± 0.19^{k}	0.9997
LSL_1.00	3.838 ± 0.039^{j}	37.65 ± 0.44^{f}	0.9999

Note: η_c − Casson plastic viscosity; τ_{OC} − Casson yield stress; PCC − Pearson correlation coefficient (for Casson model fit). The values are presented as mean ± SD of three measurements. Different superscript letters in the same column indicate statistically significant differences between the samples ($p \leq 0.05$, Tukey HSD test).

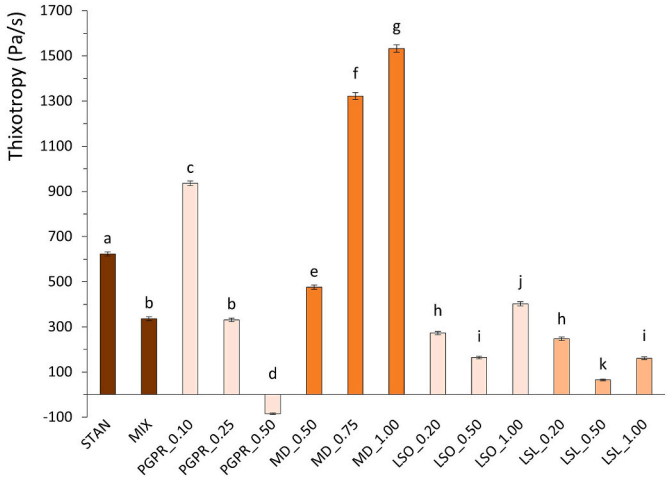

Fig. 4. Thixotropy values of chocolate samples determined by the viscometric flow ramp-up and ramp-down method. Different superscript letters above the error bars (standard deviations) indicate statistically significant differences between the samples ($p \leq 0.05$, Tukey HSD test).

PGPR_0.50 sample at shear rates exceeding 1 s^{-1}. This effect, referred to as antithixotropy, has been interpreted as a shear-induced structural build-up resulting from the formation of crosslinks (Amat Yusof et al., 2020; Buitenhuis & Pönitsch, 2003). As illustrated in Fig. 4, a substantial increase in thixotropy (from 475.79 to 1532.24 Pa/s) was observed with increasing concentrations of MD emulsifier in the chocolate. This phenomenon was attributed to the shear-induced formation of rigid local structural rearrangements within the crystal fat network (Barnes, 1997; Cahyani et al., 2019; Schantz & Rohm, 2005).

3.3. Bending properties of chocolate bars

Bending properties of the studied chocolate bars are shown in Fig. 5. The MIX sample exhibited maximum bending force (F_{max}) of 38.35 ± 0.18 N and modulus of elasticity (E_B) of 100.54 ± 14.01 MPa. The addition of emulsifiers increased both above mentioned parameters. A decrease of F_{max} from 48.81 ± 4.95 N to 32.70 ± 3.45 N was observed with increasing PGPR concentration (from 0.10 to 0.25 w.%). Such behaviour indicated successful formation of softer structure of PGPR_0.25 sample (Fig. 5A) compared to PGPR_0.10. However, the PGPR_0.50 specimen showed an increase in F_{max} to 45.69 ± 1.02 N, reflecting the increasing sample's bending stiffness. These findings were consistent with the samples' bending moduli, as shown in Fig. 5B. There was found no statistically significant differences of F_{max} and E_B for STAN and MIX samples ($p > 0.05$).

The MD_0.50 and MD_0.75 samples exhibited an increase in F_{max} and a decrease in E_B, whereas the opposite trend was observed for MD_1.00. The MD_0.50 sample recorded the highest E_B of 171.30 ± 19.80 MPa, indicating the highest mechanical stiffness among all samples studied. The LSO samples exhibited a statistically insignificant decrease in F_{max} and E_B with increasing lecithin concentration ($p > 0.05$). This effect was attributed to a reduction in the samples' bending strength. The LSL samples exhibited lower bending stiffness compared to LSO (Fig. 5). The obtained results were in an agreement with the findings of other authors (Severa, 2014; Zhao et al., 2018).

Above results confirmed that the mechanical behaviour of chocolate is closely linked with the fineness of the dispersed phase and to the emulsifier concentration. Lower $D_V(90)$ values indicate a finer and more homogeneous distribution of sugar and cocoa particles within the fat matrix, which enables a more efficient stress transfer under mechanical loading. This microstructural homogeneity was reflected in increased F_{max} and E_B, where the structure reinforcement without excessive particle aggregation can be assumed.

3.4. Acoustic properties of chocolate bars

Acoustic emissions occurred during chocolate bars fracture are known to be directly associated with the stress-induced mechanical energy accumulation in the chocolate matrix, followed by its rapid release (Kumbár et al., 2024). The lowest peak A-weighted sound pressure level L_{pAmax} value of 44.20 ± 0.85 dB was observed for the MIX sample (Fig. 6). Higher L_{pAmax} values were observed for other samples under study. This phenomenon was attributed to the formation of strong fat crystals network, hence resulting in a more rigid chocolate structure (Gregersen et al., 2016). Such fat crystal network is capable of accumulating higher mechanical energy during compression and releasing it rapidly, accompanied by sound emissions of higher intensity.

The effect was most pronounced in samples containing the MD emulsifier, which exhibited the highest L_{pAmax} values across all

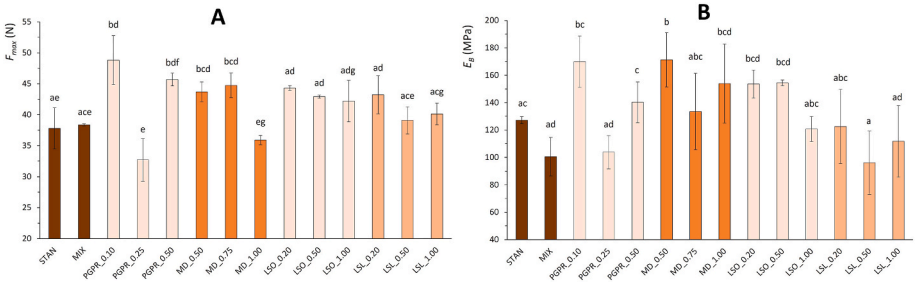

Fig. 5. Results of chocolates' maximum bending force F_{max} (part A) and modulus of elasticity E_B (part B) analysed by the three-point bending test. Different superscript letters above the error bars (standard deviations) indicate statistically significant differences between the samples ($p \leq 0.05$, Tukey HSD test).

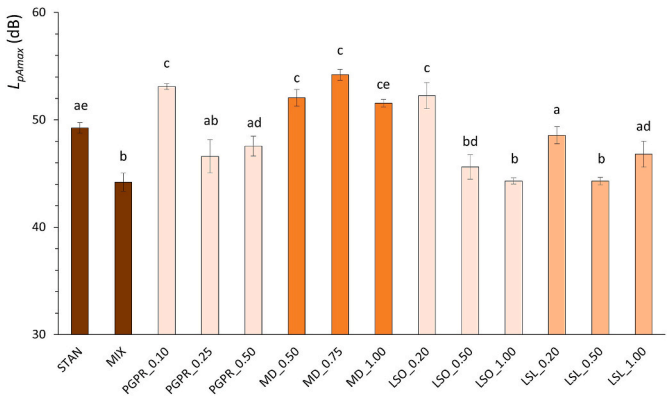

Fig. 6. Results of chocolates' acoustic properties evaluated as peak A-weighted sound pressure level L_{pAmax} (dB). Different superscript letters above the error bars (standard deviations) indicate statistically significant differences between the samples ($p \leq 0.05$, Tukey HSD test).

concentrations, indicating a more brittle and stiffer chocolate structure (Lapčíková et al., 2022). Notably, L_{pAmax} was found to increase concurrently with F_{max} values determined in bending tests (Fig. 5A). This relationship supports the earlier findings of (Gregersen et al., 2016), who reported that a harder, less flexible structure promotes more rapid energy release upon deformation, resulting in higher-intensity acoustic emissions.

3.5. Thermal properties

Melting properties of studied samples were evaluated using the onset melting temperature (T_o), peak melting temperature (T_p), and melting enthalpy (ΔH). As shown in Table 5, T_o values ranged from 26.51 °C for MD_1.00 to 27.38 °C for STAN, and T_p from 31.59 °C for PGPR_0.50 to 32.23 °C for MD_0.75, indicating the presence of stable cocoa butter polymorph V. When the concentration of emulsifier increased, the melting point of chocolate non-significantly increased ($p > 0.05$), because the emulsifier affects the crystalline structure of fat (Afoakwa, 2016). An increase in emulsifier concentration generally resulted in higher melting enthalpy values with ΔH ranging from 39.78 to 41.68 J/g (Fig. S2, Appendix A2, Supplementary Material). This indicated that emulsifiers promoted the formation of a more stable crystalline fat network (Konar et al., 2024). It can be assumed that lecithin samples coated sugar crystals at the sugar-fat interface, thereby may reduce particle-particle interactions and the number of aggregated sugar crystals dispersed in the fat phase (Dhonsi & Stapley, 2006; Vernier, 1997).

Results of the MDSC measurements are presented in Fig. 7 and summarised in Table 6. These experiments enabled detailed characterisation of the melting profiles of the chocolate samples and provided insight into the polymorphic composition of cocoa butter in studied samples. The reversing heat-flow curves describe thermodynamic melting of fat crystals (molecular rearrangement), whereas the non-reversing component reflects kinetic events occurring during melting. The combination of both signals yields the total heat-flow response (Lapčík et al., 2022).

Across all samples, the total and reversing heat-flow curves displayed a single dominant endothermic peak at the temperature of approximately 31.2 – 31.3 °C, corresponding to the melting of cocoa butter polymorphic form V (β_2). This clearly indicates that form V was the predominant crystalline structure in the analysed materials. The non-reversing heat-flow curves revealed four minor endothermic transitions associated with metastable polymorphs. These events collectively point to the presence of a mixture of forms I–IV, along with a trace amount of the most stable form VI. For the STAN, the first endotherm (T_p = 22 °C, ΔH = 0.037 J/g) was characteristic of highly metastable forms I (γ) or II (α), which melt between 17 and 23 °C and exhibit minimal enthalpy, confirming their negligible contribution. The second endotherm (T_p = 27.8 °C, ΔH = 3.92 J/g) corresponds to moderately metastable polymorphs III (β'_2) or IV (β'_1). The relatively high enthalpy in this region indicates that a significant fraction of the sample remained in these intermediate forms. A third minor transition (T_p = 31.19 °C, ΔH = 0.574 J/g) was overlapped with the main melting event. Its small enthalpy suggests partial melting of crystals undergoing transformation from form IV to form V, reflecting an active recrystallization. The fourth small peak (T_p = 34.08 °C, ΔH = 0.119 J/g) lies within the melting interval of the most stable form VI (β_1), indicating only trace amounts, likely arising from slow, long-term structural reorganisation during storage.

The comparison between the STAN and MIX samples revealed no meaningful differences in most thermal parameters. The only notable distinction occurred in the non-reversing heat flow, where the MIX sample displayed a slightly higher enthalpy for the third transition (T_p = 31.32 °C, ΔH = 0.689 J/g). This suggests that the MIX sample required more energy for crystal rearrangement, implying a marginally higher proportion of incompletely transformed intermediate polymorphs. Despite this, both samples predominantly contained form V and are therefore expected to retain favourable technological and sensory characteristics. The observed quantities of forms III–IV and VI in both samples highlight the subtle but measurable influence of storage conditions on polymorphic evolution in cocoa butter. Overall, the MDSC results confirmed that form V dominates the crystalline structure in both samples, consistent with a well-tempered cocoa butter matrix that is expected to exhibit desirable physical attributes such as gloss, hardness and sharp fracture. Nonetheless, the presence of forms III–IV and traces of form VI indicates partial ripening or recrystallization processes, potentially linked to long-term storage, while the occurrence of forms I–III is likely related to earlier episodes of rapid cooling.

The influence of emulsifiers on the thermal behaviour of cocoa butter was primarily evident in the non-reversing heat-flow signal. Emulsifiers can interfere with nucleation mechanisms, modify the kinetics of recrystallization, and stabilise otherwise unstable polymorphic forms. These effects manifest as distinct endothermic events associated with the melting or transformation of metastable structures. Certain emulsifiers were found to stabilise polymorphs III and IV, which resulted in a pronounced non-reversing endotherm within the 27–29 °C region. A finer crystallization pattern, characterised by smaller crystal domains and a higher density of structural defects, further enhances kinetic transformations, and thus increases the magnitude of the non-reversing heat-flow signal.

LSL_0.50 and PGPR_0.25 exhibited particularly strong effects. Both

Table 5
Melting properties of dark chocolate samples determined by DSC analysis in the temperature range of (5 – 50) °C.

Samples	T_o (°C)	T_p (°C)	ΔH (J/g)
STAN	27.38 ± 0.09^{a}	32.08 ± 0.07^{ab}	40.69 ± 0.06^{ag}
MIX	26.65 ± 0.08^{bcd}	31.72 ± 0.05^{ab}	40.58 ± 0.08^{ae}
PGPR_0.10	26.83 ± 0.14^{cf}	32.10 ± 0.26^{ab}	39.78 ± 0.04^{b}
PGPR_0.25	26.65 ± 0.14^{bcd}	31.95 ± 0.06^{ab}	39.95 ± 0.07^{bd}
PGPR_0.50	26.82 ± 0.01^{cf}	31.59 ± 0.19^{a}	40.29 ± 0.09^{de}
MD_0.50	26.82 ± 0.01^{cf}	31.86 ± 0.04^{ab}	40.14 ± 0.10^{de}
MD _0.75	26.86 ± 0.04^{cef}	32.23 ± 0.25^{b}	40.33 ± 0.07^{e}
MD _1.00	26.51 ± 0.03^{d}	32.11 ± 0.22^{ab}	41.23 ± 0.08^{f}
LSO_0.20	27.07 ± 0.04^{ef}	31.91 ± 0.24^{ab}	40.89 ± 0.06^{gi}
LSO_0.50	26.99 ± 0.04^{f}	31.89 ± 0.18^{ab}	41.05 ± 0.06^{fi}
LSO_1.00	26.67 ± 0.06^{bcd}	31.73 ± 0.06^{ab}	41.18 ± 0.05^{f}
LSL_0.20	26.71 ± 0.06^{bcd}	31.88 ± 0.07^{ab}	41.12 ± 0.09^{fi}
LSL_0.50	26.69 ± 0.04^{bcd}	32.15 ± 0.26^{ab}	41.36 ± 0.11^{f}
LSL_1.00	26.67 ± 0.03^{bcd}	31.91 ± 0.19^{ab}	41.68 ± 0.08^{j}

Note: T_o – onset melting temperature; T_p – peak melting temperature; ΔH – melting enthalpy. The values are presented as mean ± SD of three measurements. Different superscript letters in the same column indicate statistically significant differences between the samples ($p \leq 0.05$, Tukey HSD test).

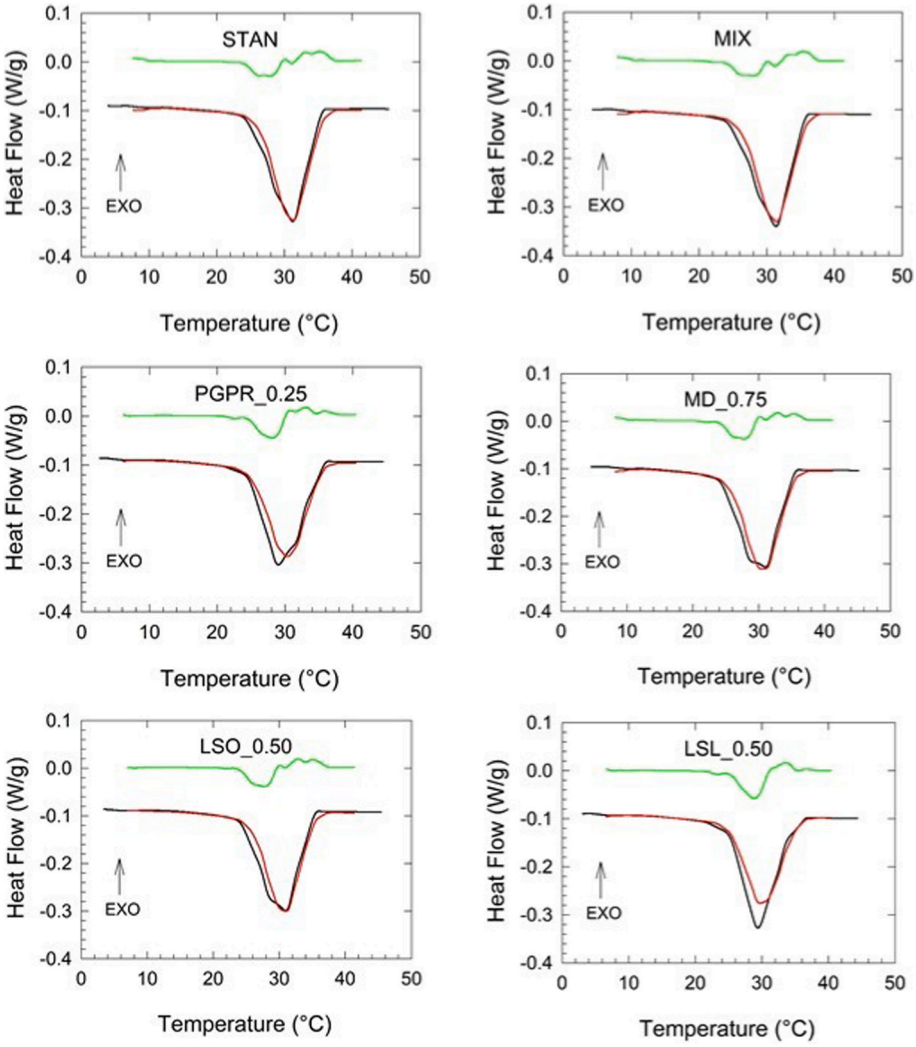

Fig. 7. Temperature modulated DSC thermograms of studied chocolate samples with detected endothermic peaks on total heat flow (black), reversing heat flow (red) and non-reversing heat flow curves (green).

emulsifiers produced an intensified endothermic peak at the temperature of approximately 28 °C, indicating the stabilization of polymorphs III/IV. Although form V ultimately developed in these samples, it arose predominantly through the transformation of metastable crystals. Consequently, the transition from forms III/IV to form V generated a markedly stronger non-reversing endotherm. In summary, PGPR and LSL promoted enhanced recrystallization activity, consistent with the increased kinetic signatures observed in the non-reversing heat-flow component.

3.6. Colour profile

Colour parameters of dark chocolate samples, including CIE $L^*a^*b^*$ coordinates, hue angle (h^*), chroma (C^*), and total colour difference (ΔE^*) are summarised in Table S1 (Appendix A3, Supplementary Material). Across all samples, the emulsifier exerted a limited effect on the colour profile, with only minor variations in lightness (L^*) and chromaticity coordinates (a^*, b^*), indicating that emulsifiers effectively maintained the visual consistency of chocolates (Sözeri Atik et al., 2020). All samples exhibited red hues, as reflected by hue angle (h^*) values in the range of approximately (25 – 40°), accompanied by relatively high colour saturation (C^*). The blending process (MIX) led to only *weakly perceptible* colour difference relative to the STAN sample ($\Delta E^* = 1.10$), suggesting a negligible impact of mixing on colour parameters. The selection of emulsifier caused slight variations in the chocolate colour profile. Samples containing PGPR and lecithins (LSO, LSL) showed mostly *weakly perceptible* colour differences ($\Delta E^* \cong 0.6 – 1.8$), as presented in Table S1. For LSO_0.20 sample, an *imperceptible* colour difference ($\Delta E^* < 0.20$) was observed. Notably, the application of MD emulsifier at higher concentrations resulted in statistically significant decrease in lightness ($p \leq 0.05$, Tukey test), rendering the chocolates visually darker than other formulations. This reduction in L^* may be attributed to the interaction between the lipophilic emulsifier and fat-based components, likely reducing the light reflection. Furthermore, the samples with MD displayed distinctive changes in b^* and h^* parameters, reflecting a minor colour shift towards yellow tones. The changes in MD colour contributed to the highest observed ΔE^* values (Table S1), which are considered *medium* colour difference (Brainard, 2003). In contrast, the MIX and STAN samples exhibited more neutral and less saturated colour profiles compared to those of the emulsified samples.

3.7. Sensory characteristics

The average sensory attribute scores of tested samples are shown in Fig. 8. Attributes assessed included chocolate colour, surface, hardness, melting in the mouth, flavour, aroma, and overall acceptance. Statistically, no significant differences were observed among the samples ($p >$

Table 6
MDSC parameters of studied chocolate samples. Applied heating rate of 2 °C/min in the temperature range from 0 to 50 °C.

Samples	MDSC heat-flow patterns								
	Total			Non-reversing			Reversing		
	T_o (°C)	T_p (°C)	ΔH (J/g)	T_o (°C)	T_p (°C)	ΔH (J/g)	T_o (°C)	T_p (°C)	ΔH (J/g)
STAN	25.44	31.23	44.63	20.89	22.00	0.04	26.11	31.34	42.75
				24.11	27.84	3.92			
				30.23	31.19	0.57			
				33.26	34.08	0.12			
MIX	25.38	31.36	45.43	20.99	22.09	0.03	26.09	31.47	42.34
				24.22	27.94	3.55			
				30.30	31.32	0.69			
				33.43	34.20	0.06			
PGPR_0.25	24.37	29.02	44.31	21.19	22.50	0.12	25.38	30.34	39.92
				24.69	28.18	5.75			
				30.90	31.60	0.13			
				33.49	34.49	0.31			
MD_0.75	24.90	31.01	44.57	20.88	22.05	0.05	25.74	30.49	41.66
				24.24	27.81	4.94			
				30.34	31.18	0.35			
				33.14	34.06	0.22			
LSO_0.50	25.00	30.96	43.14	20.79	21.93	0.04	25.81	31.04	40.54
				24.11	27.70	4.78			
				30.28	31.06	0.29			
				33.07	33.94	0.16			
LSL_0.50	24.63	29.41	42.60	21.84	23.21	0.18	25.05	29.69	36.09
				25.33	28.84	6.17			
				31.56	32.25	0.02			
				33.99	34.97	0.42			

Note: T_o – onset melting temperature; T_p – peak melting temperature; ΔH – melting enthalpy.

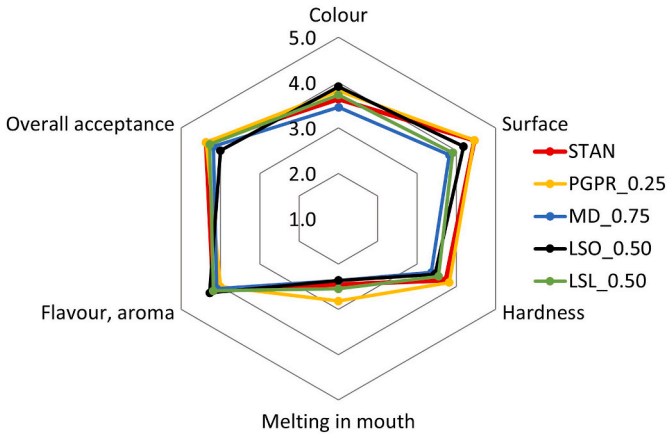

Fig. 8. Sensory mean scores for selected attributes of standard chocolate (STAN) and chocolates with different emulsifiers (at medium concentration level), using the 5-point intensity scale. Samples are represented by colour lines, as depicted in the legend.

0.05, Friedman test). Scores ranged from 3.45 to 3.91 for colour, 3.82 to 4.45 for surface, 3.36 to 3.82 for hardness, 2.36 to 2.82 for melting in the mouth, 4.00 to 4.27 for flavour and aroma, and from 4.00 to 4.36 for overall acceptance. For colour, surface, hardness, and melting in the mouth, panellists showed a preference for PGPR_0.25, while MD_0.75 was rated least favourably. Flavour and aroma scores were higher in lecithin-containing samples LSO_0.50 (4.27) and LSL_0.50 (4.18), suggesting a refined balance in these attributes and enhanced organoleptic acceptability (Mohd Hassim et al., 2024; Srinu et al., 2021). The highest overall acceptance scores were recorded for PGPR_0.25 and STAN (both 4.36), followed closely by LSL_0.50 (4.27), indicating a general preference for these samples. By ranking tests, no significant differences in textural or overall preferences among the samples were observed, except between the STAN, which had the highest preferences, and MD_0.75, showing the lowest preferences ($p \leq 0.05$, Nemenyi test).

3.8. Principal component analysis

The principal component analysis (PCA) demonstrated that the first two principal components (PC1 and PC2) accounted for 73.24% of the total data variance, with PC1 explaining 47.83% and PC2 25.40%. As presented in Fig. S3A (Appendix A4, Supplementary Material), a higher positive correlation was found between bending parameters (modulus of elasticity E_B, maximum bending force F_{max}) and sound pressure level (L_{pAmax}) showing that acoustic emissions of chocolate bars proportionally increase with the bending rigidity. On the other side, weak correlations (from −0.10 to 0.04) were determined between flow attributes (Casson plastic viscosity η_c, yield stress τ_{0C}) and L_{pAmax} indicating that the rheological behaviour of molten chocolate was marginally related to the acoustic properties of solid chocolate samples. Nonetheless, the Casson plastic viscosity had a medium negative correlation with F_{max} (−0.45) and E_B (−0.40) suggesting an indirect proportion between chocolate flow and bending stiffness.

PC1 was primarily dominated by moderate positive loadings from E_B (0.5811), F_{max} (0.5173), and L_{pAmax} (0.4809), alongside a negative contribution from η_c (−0.3942). These associations suggest that PC1 includes a dimension of mechanical rigidity and flow behaviour, where chocolates exhibiting higher bending strength with relation to higher acoustic emissions tend to possess lower plastic viscosity. This was particularly relevant for PGPR_0.10, MD_0.50 and LSO_0.20 samples, positioned in the same PCA cluster, as can be seen in Fig. S3B (Appendix A4, Supplementary Material). Conversely, samples with elevated η_c from a different cluster (PGPR_0.25, STAN and MIX) were positioned more negatively along PC1 axis, reflecting their reduced mechanical stiffness (F_{max}, E_B). It follows that PC1 reflects a balance between solid-like mechanical properties of chocolate bars and viscous flow characteristics of molten chocolate.

PC2, which explains 25.40% of the data variance, was driven by a stronger positive loading from yield stress (0.7517), accompanied by negative contributions from Casson plastic viscosity (−0.5440) and L_{pAmax} (−0.3384). Yield stress prominence on PC2 axis, represented by a nearly perpendicular vector in the PCA space (Fig. S3C, Appendix A4, Supplementary Material), suggests that the PC2 component was closely

tied to the flow resistance of molten chocolate. Along PC2 axis, LSO_1.00 sample showed particularly higher τ_{0C}, being associated with the samples of similarly lower elasticity (LSL_1.00, LSL_0.50) to the same cluster (Fig. S3B and S3C). Weak loadings from modulus of elasticity (−0.1350) and maximum bending force (−0.0792) imply that PC2 was not significantly affected by the aspects of mechanical rigidity. However, negative loadings from η_c (−0.5440) indicate that PC2 reflects chocolate plastic deformation and structural response under flow stress. These relations suggest that chocolates with varying η_c and lower τ_{0C} occupy unique positions in the negative PC2 segments, as observed for PGPR samples (Fig. S3C, Appendix A4, Supplementary Material).

4. Conclusion

Present study systematically investigated the effect of the post-conching blending step accompanied with the application of selected emulsifiers at different concentrations on the chocolate fat phase organisation. It was found that the applied emulsifiers modulated specific fat-sugar particle interactions, fat phase structuring, and matrix interfacial behaviour, resulting in measurable variations in physico-mechanical properties of studied chocolates. It was found, that the blending process reduced both thixotropy and Casson plastic viscosity and simultaneously increased yield stress. Lecithin-based emulsifiers generally increased yield stress and reduced Casson plastic viscosity, most likely due to their multilayer adsorption on solid particles surfaces. This led to the consequent interparticle lubrication effects. At LSL and LSO lecithins concentrations of 0.20 and 0.50 w.%, a decrease in plastic viscosity was observed, whereas at 1.00 w.% the trend reversed and plastic viscosity was increased. PGPR facilitated at 0.10 and 0.25 w.%. concentrations the liquefaction of the chocolate and exhibited concentration-dependent effects on chocolate bars bending and acoustic properties during fracture. A distinct behaviour was observed at 0.50 w.%. MD modified chocolate samples displayed increased structural rigidity attributed to its interactions with the surrounding fat phase. Enhanced matrix cohesion and mechanical integrity correlated well with the decreasing chocolate particle size. Acoustic emissions corroborated these findings, indicating that the mechanical response and brittleness of the chocolate matrix varied according to emulsifier applied, with MD samples demonstrating increased L_{pAmax} values.

DSC analysis revealed no statistically significant differences in peak melting temperatures, indicating no significant effect on the crystallization of cocoa butter in a stable modification V. Although, higher emulsifier concentrations led to an increase in melting enthalpy of cocoa butter matrix. Blending experiments with emulsifiers showed that lecithins, particularly sunflower lecithin (LSL), promote a more amorphous internal structure, as evidenced by the higher phase transition enthalpies observed in the non-reversible heat-flow signal during MDSC analysis. Chocolates containing PGPR or the MD emulsifier exhibited increased mechanical stiffness. These findings were further supported by reduced non-reversible heat in MDSC. An increase in moisture content following blending was observed in chocolates containing PGPR and MD. The associated rise in firmness was primarily attributed with the moisture-induced sucrose particles surface dissolution, followed by their localised recrystallization and agglomeration. These processes produce a coarser particle dispersion, elevate interparticle friction and partially destabilise the fat matrix, collectively resulting in greater apparent stiffness of the chocolate mass. Colour analysis showed that emulsifier addition induced subtle alterations in lightness, chromaticity, and hue angle, particularly for MD and lecithin emulsifiers. Sensory evaluation revealed no significant differences in overall acceptance among the samples. However, higher preferences were rated for samples containing PGPR and LSL.

Multivariate analysis highlighted coherent correlations between plastic viscosity, fracture behaviour, acoustic response and sensory attributes, providing a compact map of how different emulsifier strategies shift chocolate behaviour along practical axes such as ease of processing versus crispness of bite.

Although this study provides a systematic evaluation of how emulsifier type and concentration affect the functional properties of blended dark chocolate, several limitations should be considered: (1) the mixing step was examined under a single processing condition; (2) the emulsifier specifications provided only by the suppliers were available; (3) the study proposes mechanistic explanations related to emulsifier interactions and fat phase organization, although no XRD measurements were performed. MDSC was used as an alternative method to detect the polymorphic transformation of cocoa butter.

CRediT authorship contribution statement

Barbora Lapčíková: Writing – review & editing, Writing – original draft, Visualization, Validation, Supervision, Resources, Project administration, Methodology, Investigation, Funding acquisition, Formal analysis, Data curation, Conceptualization. **Lubomír Lapčík:** Writing – review & editing, Writing – original draft, Visualization, Resources, Funding acquisition, Formal analysis, Conceptualization. **Vojtěch Neuwirth:** Writing – review & editing, Writing – original draft, Validation, Software, Methodology, Investigation, Data curation, Conceptualization. **Erick Omodho Okelo:** Writing – review & editing, Writing – original draft, Validation, Software, Methodology, Data curation. **Tomáš Valenta:** Writing – original draft, Visualization, Validation, Formal analysis, Data curation. **Martin Vašina:** Writing – review & editing, Writing – original draft, Validation, Methodology, Investigation, Data curation. **David Řepka:** Validation, Investigation, Data curation. **Aneta Machalová:** Visualization, Validation, Investigation, Data curation.

Ethical approval

All participants of sensory panel gave their informed consent to take part in the study and use their information.

Funding

This work was supported by the Tomas Bata University in Zlín (grant number IGA/FT/2025/007), and the Palacky University in Olomouc (grant number IGA_PrF_2026_012).

Declaration of competing interest

The authors declare that they have no known competing financial interests or personal relationships that could have appeared to influence the work reported in this paper.

Appendix A. Supplementary data

Supplementary data to this article can be found online at https://doi.org/10.1016/j.lwt.2026.119206.

Data availability

Data will be made available on request.

References

Afoakwa, E. O. (2016). *Chocolate science and technology*. Hoboken, NJ: John Wiley & Sons. https://doi.org/10.1002/9781118913758

Afoakwa, E. O., Paterson, A., & Fowler, M. (2007). Factors influencing rheological and textural qualities in chocolate – A review. *Trends in Food Science & Technology, 18*(6), 290–298. https://doi.org/10.1016/j.tifs.2007.02.002

Albak, F., & Tekin, A. R. (2016). Variation of total aroma and polyphenol content of dark chocolate during three phase of conching. *Journal of Food Science and Technology-Mysore, 53*(1), 848–855. https://doi.org/10.1007/s13197-015-2036-4

Amat Yusof, F. A., Yamaki, M., Kawai, M., Okajima, M. K., Kaneko, T., & Mitsumata, T. (2020). Rheopectic behavior for aqueous solutions of megamolecular polysaccharide sacran. *Biomolecules, 10*(1), 155. https://doi.org/10.3390/biom10010155

Anicic, O., Petković, D., & Cvetkovic, S. (2016). Evaluation of wind turbine noise by soft computing methodologies: A comparative study. *Renewable and Sustainable Energy Reviews, 56*, 1122–1128. https://doi.org/10.1016/j.rser.2015.12.028

Barnes, H. A. (1997). Thixotropy—A review. *Journal of Non-newtonian Fluid Mechanics, 70*(1), 1–33. https://doi.org/10.1016/S0377-0257(97)00004-9

Bastida-Rodríguez, J. (2013). The food additive polyglycerol polyricinoleate (E-476): Structure, applications, and production methods. *International Scholarly Research Notices, 2013*(1), Article 124767. https://doi.org/10.1155/2013/124767

Beckett, S. T. (2008). *The science of chocolate*. Cambridge, UK: The Royal Society of Chemistry. https://doi.org/10.1039/9781847558053

Beckett, S. T., Fowler, M. S., & Ziegler, G. R. (2017). *Beckett's industrial chocolate manufacture and use*. Chichester, UK: Wiley Blackwell.

Bhandari, M., Bobade, H., Sharma, R., & Sharma, S. (2025). Mixing, blending, and emulsification in processing. In *Anonymous engineering solutions for sustainable food and dairy production: Innovations and techniques in food processing and dairy engineering* (pp. 231–260). Cham, Switzerland: Springer.

Biswas, N., Cheow, Y. L., Tan, C. P., & Siow, L. F. (2017). Physical, rheological and sensorial properties, and bloom formation of dark chocolate made with cocoa Butter substitute (CBS). *LWT, 82*, 420–428. https://doi.org/10.1016/j.lwt.2017.04.039

Brainard, D. H. (2003). Color appearance and color difference specification. In S. K. Shevell (Ed.), *The science of color* (pp. 191–216). Amsterdam, Netherlands: Elsevier.

Buitenhuis, J., & Pönitsch, M. (2003). Negative thixotropy of polymer solutions. 1. A model explaining time-dependent viscosity. *Colloid and Polymer Science, 281*(3), 253–259. https://doi.org/10.1007/s00396-002-0768-y

Cahyani, A., Kurniasari, J., Nafingah, R., Rahayoe, S., Harmayani, E., & Saputro, A. D. (2019). Determining casson yield value, casson viscosity and thixotropy of molten chocolate using viscometer. *IOP Conference Series: Earth and Environmental Science, 355*(1), Article 012041. https://doi.org/10.1088/1755-1315/355/1/012041

Caparosa, M. H., & Hartel, R. W. (2020). Characterizing lecithin interactions in chocolate using interfacial properties and rheology. *Journal of the American Oil Chemists' Society, 97*(12), 1309–1317. https://doi.org/10.1002/aocs.12419

Dhonsi, D., & Stapley, A. G. F. (2006). The effect of shear rate, temperature, sugar and emulsifier on the tempering of cocoa butter. *Journal of Food Engineering, 77*(4), 936–942. https://doi.org/10.1016/j.jfoodeng.2005.08.022

Gallery, C., Bourge, S., & Agoda-Tandjawa, G. (2024). Flow behaviors of multiple molten chocolate matrices: Appropriate curve fitting models and impact of different types of surfactants. *Journal of Food Engineering, 363*, Article 111780. https://doi.org/10.1016/j.jfoodeng.2023.111780

Garti, N., & Aserin, A. (2012). Effect of emulsifiers on cocoa butter and chocolate rheology, polymorphism, and bloom (chapter 12). In N. Garti, & N. R. Widlak (Eds.), *Cocoa butter and related compounds* (pp. 275–305). Urbana, Illinois, USA: AOCS Press.

Glicerina, V., Balestra, F., Dalla Rosa, M., & Romani, S. (2016). Microstructural and rheological characteristics of dark, milk and white chocolate: A comparative study. *Journal of Food Engineering, 169*, 165–171. https://doi.org/10.1016/j.jfoodeng.2015.08.011

Gómez-Fernández, A. R., Faccinetto-Beltrán, P., Orozco-Sánchez, N. E., Perez-Carrillo, E., Santacruz, A., & Jacobo-Velázquez, D. A. (2021). Physicochemical properties and sensory acceptability of sugar-free dark chocolate formulations added with probiotics. *Revista Mexicana de Ingenieria Quimica, 20*(2), 697–709. https://doi.org/10.24275/rmiq/Alim2131

Gregersen, S. B., Povey, M. J. W., Andersen, M. D., Hammershøj, M., Rappolt, M., Sadeghpour, A., & Wiking, L. (2016). Acoustic properties of crystallized fat: Relation between polymorphic form, microstructure, fracturing behavior, and sound intensity. *European Journal of Lipid Science and Technology, 118*(9), 1257–1270. https://doi.org/10.1002/ejlt.201500435

Guckenbiehl, Y., Romero, A., Haug, H., Ortner, E., Rothkopf, I., Schweiggert-Weisz, U., Buettner, A., & Gola, S. (2024). Conching of dark chocolate - Processing impacts on aroma-active volatiles and viscosity of plastic masses. *Current Research in Food Science, 9*. https://doi.org/10.1016/j.crfs.2024.100909

Indiarto, R., Situmorang, A., Harunaningtyas, A., Arifin, H. R., Subroto, E., Herawati, E., Djali, M., & Muhammad, D. (2024). Reformulation of white chocolate with Soy- and coconut-based vegetable ingredients incorporating encapsulated cinnamon extract: Investigation of physicochemical, antioxidant, and sensory properties. *International Journal of Food Properties, 27*(1), 704–728. https://doi.org/10.1080/10942912.2024.2355904

International Organization for Standardization. (1998). *ISO standard no. 14125:1998. fibre-reinforced plastic composites - Determination of flexural properties* (p. 18). Geneva, Switzerland: International Organization for Standardization.

International Organization for Standardization. (2023). *ISO standard no. 8586:2023. Sensory analysis - Selection and training of sensory assessors* (p. 38). Geneva, Switzerland: International Organization for Standardization.

Kadivar, S., De Clercq, N., Mokbul, M., & Dewettinck, K. (2016). Influence of enzymatically produced sunflower oil based cocoa butter equivalents on the phase behavior of cocoa butter and quality of dark chocolate. *LWT, 66*, 48–55. https://doi.org/10.1016/j.lwt.2015.10.006

Konar, N., Palabiyik, I., Karimidastjerd, A., & Said Toker, O. (2024). Chocolate microstructure: A comprehensive review. *Food Research International, 196*, Article 115091. https://doi.org/10.1016/j.foodres.2024.115091

Kumbár, V., Trnka, J., Kouřilová, V., Dufková, R., Votava, J., Čupera, J., Nedomová, Š., Hřivna, L., & Buchar, J. (2024). Stress wave attenuation in chocolate. *Journal of Food Engineering, 374*, Article 112037. https://doi.org/10.1016/j.jfoodeng.2024.112037

Lapčík, L., Lapčíková, B., Gautam, S., Vašina, M., Valenta, T., Řepka, D., Čépe, K., & Rudolf, O. (2022). Acoustic and mechanical testing of commercial cocoa powders. *International Journal of Food Properties, 25*(1), 2184–2197. https://doi.org/10.1080/10942912.2022.2127760

Lapčíková, B., Lapčík, L., Salek, R., Valenta, T., Lorencová, E., & Vašina, M. (2022). Physical characterization of the milk chocolate using whey powder. *LWT, 154*, Article 112669. https://doi.org/10.1016/j.lwt.2021.112669

Lapčíková, B., Lapčík, L., Valenta, T., & Chvatíková, M. (2024). Plant-based emulsions as dairy cream alternatives: Comparison of viscoelastic properties and colloidal stability of various model products. *Foods, 13*(8), 1225. https://doi.org/10.3390/foods13081225

Leyva-Porras, C., Cruz-Alcantar, P., Espinosa-Solís, V., Martínez-Guerra, E., Pinon-Balderrama, C. I., Martínez, I. C., & Saavedra-Leos, M. Z. (2020). Application of differential scanning calorimetry (DSC) and modulated differential scanning calorimetry (MDSC) in food and drug industries. *Polymers, 12*(1). https://doi.org/10.3390/polym12010005

Mohd Hassim, N. A., Kanagaratnam, S., Tang, T. K., & Sofian Seng, N. S. (2024). The effect of sunflower wax and carnauba wax on the storage stability and sensory evaluation of palm-based chocolate spread. *Grasas Y Aceites, 75*(3), 2193. https://doi.org/10.3989/gya.0651241.2193

Muhammad, D., Saputro, A. D., Rottiers, H., Van de Walle, D., & Dewettinck, K. (2018). Physicochemical properties and antioxidant activities of chocolates enriched with engineered cinnamon nanoparticles. *European Food Research and Technology, 244*(7), 1185–1202. https://doi.org/10.1007/s00217-018-3035-2

Neuwirth, V., Lapčíková, B., Lapčík, L., Valenta, T., & Míšková, Z. (2024). Effect of technological processing and recipe formulation on the physico-chemical properties of ganaches and chocolate pralines. *Journal of Food Engineering, 378*, Article 112124. https://doi.org/10.1016/j.jfoodeng.2024.112124

Pombal, M., Marcet, I., Rendueles, M., & Diaz, M. (2024). Emulsifiers: Their influence on the rheological and texture properties in an industrial chocolate. *Molecules, 29*(21). https://doi.org/10.3390/molecules29215185

Rohm, H., Böhme, B., & Skorka, J. (2018). The impact of grinding intensity on particle properties and rheology of dark chocolate. *LWT-Food Science and Technology, 92*, 564–568. https://doi.org/10.1016/j.lwt.2018.03.006

Saputro, A. D., Van de Walle, D., Aidoo, R. P., Mensah, M. A., Delbaere, C., De Clercq, N., Van Durme, J., & Dewettinck, K. (2017). Quality attributes of dark chocolates formulated with palm sap-based sugar as nutritious and natural alternative sweetener. *European Food Research and Technology, 243*(2), 177–191. https://doi.org/10.1007/s00217-016-2734-9

Saputro, A. D., Van de Walle, D., Kadivar, S., Mensah, M. A., Van Durme, J., & Dewettinck, K. (2017). Feasibility of a small-scale production system approach for palm sugar sweetened dark chocolate. *European Food Research and Technology, 243*(6), 955–967. https://doi.org/10.1007/s00217-016-2812-z

Schantz, B., & Rohm, H. (2005). Influence of lecithin–PGPR blends on the rheological properties of chocolate. *LWT, 38*(1), 41–45. https://doi.org/10.1016/j.lwt.2004.03.014

Servais, C., Ranc, H., & Roberts, I. D. (2003). Determination of chocolate viscosity. *Journal of Texture Studies, 34*(5-6), 467–497. https://doi.org/10.1111/j.1745-4603.2003.tb01077.x

Severa, L. (2014). Deformation and fracture properties of dark chocolate. *Acta Universitatis Agriculturae et Silviculturae Mendelianae Brunensis, 56*(2), 115–122. https://doi.org/10.11118/actaun200856020115

Sözeri Atik, D., Bölük, E., Toker, O. S., Palabiyik, I., & Konar, N. (2020). Investigating the effects of Lecithin-PGPR mixture on physical properties of milk chocolate. *LWT, 129*, Article 109548. https://doi.org/10.1016/j.lwt.2020.109548

Srinu, D., Baskaran, D., & Ramesh, S. (2021). Sensory evaluation, textural parameters and microbial analysis of chocolate incorporated with spices. *The Pharma Innovation Journal, 10*(5), 550–553.

Staiano, M. A. (2007). Age-weighted sound levels. *Noise Control Engineering Journal, 55*(5), 446–456. https://doi.org/10.3397/1.2790526

Suri, T., & Basu, S. (2022). Heat resistant chocolate development for subtropical and tropical climates: A review. *Critical Reviews in Food Science and Nutrition, 62*(20), 5603–5622. https://doi.org/10.1080/10408398.2021.1888690

Toker, O. S., Ozonuk, S., Gunes, R., Icyer, N. C., Rasouli, H. P., Konar, N., Palabiyik, I., & Altop, C. (2024). Importance of emulsifiers in chocolate industry: Effect on structure, machinability, and quality of intermediate and final products. *Journal of the American Oil Chemists' Society, 101*(8), 721–733. https://doi.org/10.1002/aocs.12829

Toker, O. S., Palabiyik, I., & Konar, N. (2019). Chocolate quality and conching. *Trends in Food Science & Technology, 91*, 446–453. https://doi.org/10.1016/j.tifs.2019.07.047

Tolstorebrov, I., Eikevik, T. M., & Bantle, M. (2014). A DSC determination of phase transitions and liquid fraction in fish oils and mixtures of triacylglycerides. *Food Research International, 58*, 132–140. https://doi.org/10.1016/j.foodres.2014.01.064

Vavreck, A. N. (2004). Flow of molten milk chocolate from an efflux viscometer under vibration at various frequencies and displacements. *International Journal of Food*

Science and Technology, 39(4), 465–468. https://doi.org/10.1111/j.1365-2621.2004.00805.x

Vernier, F. C. (1997). *Influence of emulsifiers on the rheology of chocolate and suspensions of cocoa or sugar particles in oil*. Reading, Berkshire, UK: University of Reading.

Zhao, H., Li, B., & James, B. J. (2018). Structure-fracture relationships in chocolate systems. *LWT, 96*, 281–287. https://doi.org/10.1016/j.lwt.2018.05.045

Ziegler, G. R., Garbolino, C., & Coupland, J. (2003). The influence of surfactants and moisture on the colloidal and rheological properties of model chocolate dispersions. *3rd International Symposium on Food Rheology and Structure, 3*, 335–339.

Ziegler, G. R., & Hogg, R. (2009). Particle size reduction. In S. T. Beckett (Ed.), *Industrial chocolate manufacture and use* (pp. 142–168). Chichester, West Sussex, UK: Wiley-Blackwell.